Pure appl. geophys. 162 (2005) 373–407
0033–4553/05/020373–35
DOI 10.1007/s00024-004-2606-2



Pure and Applied Geophysics

# The Permeability of an Intact Granite

A. P. S. Selvadurai[1], M. J. Boulon[2] and T. S. Nguyen

*Abstract* — The permeability of intact Barre granite is determined by conducting transient hydraulic pulse tests that induce radial flow in saturated granite cylinders containing a water-filled co-axial cavity. Saturated specimens of granite are also subjected to uniform heating on the outer cylindrical surface and the permeability of the granite is measured at the termination of a heating sequence. The theoretical basis for the use of simplified analytical solutions for evaluating the decay of the pressure pulse is examined and the permeability of the granite in the pre-heating and post-heating states is inferred from the results of pulse tests. The reported investigations document one of the limited numbers of large-scale laboratory tests conducted to determine the permeability characteristics of intact granite. The results of the permeability measurements indicate the absence of any appreciable influences of micro structural alterations in the fabric of the granite due to its heating in a saturated condition, at an average temperature of 140 °Celsius.

**Key words:** Permeability, pulse tests, transient radial flow tests, Barre granite, analysis of finite boundary effects, elastic drive equation.

## *Introduction*

The key physical property of rock that influences the movement of fluids in intact rock is its *permeability*. High pore fluid pressures that accompany mechanical and thermal loadings are usually associated with the low matrix permeability of rock masses. Despite its potential importance, the measurement and interpretation of the permeability characteristics of low permeability intact rocks is far from routine. The permeability of intact rock can be influenced by the choice of scale for the measurement of permeability, ranging from *crustal scales* of 0.5 km to 5.0 km, to *borehole scales* ranging from 30 m to 300 m, to *laboratory scales* of 5 cm to 15 cm. The "*bulk permeability*" of geological media will be influenced by the choice of scale, and factors contributing to such variations can occur due to the abundance of fractures, fissures, inclusions and other inhomogeneities.

[1] Department of Civil Engineering and Applied Mechanics, McGill University, Montréal, QC, Canada H3A 2K6. E-mail: Patrick.selvadurai@mcgill.ca

[2] Laboratoire des Sols, Solides, Structures, Université Joseph Fourier, 38000 Grenoble Cedex, France

[3] Wastes and Impacts Division, Canadian Nuclear Safety Commission, Ottawa, ON., Canada K1P 5S9

The motivation for the present work stems from the potential use of deep geological formations for the disposal of heat-emitting nuclear fuel wastes. In the context of deep geological settings, similar to those advocated by countries such as Canada, Sweden, France, Switzerland and the U.K., the natural geological medium is considered to be a vital part of the multi-barrier system which will attenuate the radionuclide migration (e.g., LAUGHTON *et al.*,1986; CHAPMAN and MCKINLEY, 1987; GNIRK, 1993; JOHNSON *et al.*, 1994a,b; SIMMONS and BAUMGARTNER, 1994). In a natural geological setting, groundwater is the primary medium for the transport of radionuclides that could be released to the environment with the eventual degradation of the nuclear waste containers. The rates of groundwater movement in a natural geological setting will depend on the *in situ* permeability and other transport characteristics of the medium. With certain intact granitic rocks, the permeability and other transport characteristics are controlled by low aspect ratio microcracks that form the pore structure network of the medium. For example, the types of microcracks occurring in granite include intragranular cracks in all three major minerals, coincident grain boundary cracks and transgranular cracks. In Westerly granite, for example, all three types of cracks are present, although their lengths rarely exceed the grain size. The various types of cracks can join together to form networks that produce pathways for fluid flow through the *intact rock*.

Most deep geological repositories that will store the heat-emitting waste are expected to experience a thermal pulse as a result of the radioactive decay. In many instances, peak temperatures of the order of 100 °C are expected to influence the Thermo-Hydro-Mechanical (THM) behavior of the rock. The largest changes in stresses are expected to occur as a result of the *relative thermal expansion* between the pore fluid and the porous rock and the time-lag associated with the dissipation of the generated pore pressures. These processes can be further influenced by geochemical interactions between the groundwater and the rock. For example, MOORE *et al.* (1983) presented results of experiments where water was passed at a low rate through cylinders of Barre and Westerly granite, subjected to temperature gradients. They observed the dissolution of minerals near the heat source and their deposition in the cooler regions. In this sense, the presence of heating is considered to have a beneficial effect on reducing the permeability of the granitic material. The experimental work of VAUGHN (1989) also confirms these findings. It is, however, recognized that intact deep geological formations that permit groundwater migration through the rock fabric, are a rarity and that the migration of radionuclides to the ground surface is likely to be through either individual fractures or through a network of widely spaced fractures. Even in the context of flow in fractures, the ability of the matrix to participate in the overall flow process becomes important to the accurate modelling of THM processes in a fractured medium (e.g., a leakage factor for the fracture, BERKOWITZ, 1989). For example, with ''tight'' or ''closed'' fractures, the flow rates in the fracture could, in some instances, be only an order of magnitude higher than that in the intact matrix. In these circumstances, the assessment of the flow through the

matrix should be taken into consideration to develop a realistic assessment of the permeability of the fracture. A similar situation can arise in evaluating the efficiency of sealing fractures using grouting and epoxy injection techniques. In such situations, the fluid transport through the sealant and the sealant-rock interface can be comparable to the fluid transport through the intact rock matrix. In recent years, considerable research effort has been directed to the conceptualization, mathematical modelling, computational modelling, laboratory experimentation and field verification of THM processes in geological media. Accounts of these and references to further work can be found in the articles and texts by TSANG (1987, 1991), BEAR *et al.* (1993), JING *et al.* (1993, 1994, 1999), STEPHANSSON (1995), SELVADURAI and NGUYEN (1995, 1996), NGUYEN and SELVADURAI (1995, 1998), COUSSY (1995), AHOLA (1995), SELVADURAI (1996a), STEPHANSSON *et al.* (1996), NIELD and BEJAN (1999) and KUMPEL (2000). In many THM models with potential for applicability to deep rock repositories, both the porosity and the intact permeability of the rock are required as input parameters.

The theoretical and experimental study of the permeability characteristics of intact rock and other low permeability geomaterials has been the subject of extensive studies conducted over the past three decades. The most notable of these studies is the seminal laboratory investigation carried out by Brace *et al.* (1968) to determine the permeability characteristics of Westerly granite. To these could be added the investigations by KNUTSON and BOHOR (1963), DAW (1971), ZOBACK and BYERLEE (1975), BRACE (1978), SUMMERS *et al.* (1978), CARLSSON and OLSSON (1979), KRANTZ *et al.* (1979), TRIMMER *et al.* (1980), MORROW *et al.* (1981), HEYSTEE and ROEGIERS (1981), HSIEH *et al.* (1981), VITOVTOVA and SHMONOV (1982), HAIMSON and DOE (1983), ZONOV *et al.* (1989), ZARAISKY and BALASHOV (1994), SHMONOV *et al.* (1994) and HEILAND (2003) who have examined the influences of a variety of factors, including pressure, stress state and temperature, on the permeability of intact crystalline rocks. Of related interest are investigations conducted to measure permeability of other low- permeability construction materials such as concrete and cement grout (POON *et al.*, 1986; BANTHIA and MINDESS, 1989; AHMED *et al.*, 1991; SELVADURAI and CARNAFFAN, 1997). The literature dealing with the assessment of the permeability characteristics of porous media is vast and no attempt will be made to provide a comprehensive list. Informative accounts are given by DAVIS (1969), BRACE (1980), DULLIEN (1992), in the compendium by HUDSON (1993) and in the article by OELKERS (1996).

The measurement of the fluid flow characteristics of low permeability geological materials can, in principle, be done either by using *steady–state flow tests* or *transient flow tests*. When the geological material has a very low permeability (i.e., in the range $10^{-18}$ m$^2$ to $10^{-24}$ m$^2$) either method requires the application of differential fluid pressures to the sample. The limiting values of the fluid pressures are governed by the strength and fracture characteristics of the material skeleton at the pore scale. For very low permeability materials, the flow rates that can be established with falling

head-type devices are extremely small and the accurate measurement of a steady flow rate is a difficult exercise. For this reason the measurement of the permeability of intact geological materials with low permeability is done by appeal to transient tests, where the decay of a pressure pulse applied on a surface of the porous medium as the fluid migrates through it, is used to evaluate the permeability characteristics. The work of BRACE *et al.* (1968) documents a one-dimensional *pulse test* in which axial flow takes place through a cylindrical sample contained between two pressurized chambers. The application of pulse tests for the evaluation of the *in situ* permeability characteristics of geological formations has received considerable attention. In these types of tests, a section of a borehole containing either an intact region of the rock mass or a fracture is pressurized using a packer system. The decay of the pressure within the borehole cavity is then used to estimate the permeability characteristics of the geological medium. Both theoretical and experimental studies related to pulse tests are given by COOPER *et al.* (1967), WANG *et al.* (1977), PAPADOPULOS *et al.* (1973), HSIEH *et al.* (1981), HODGKINSON and BARKER (1985), RUTQUIST (1995), REHBINDER (1996a,b), BUTLER Jr. (1998) and WU and PRUESS (2000). Studies by CHAPUIS (1998) and CHAPUIS and CHENAF (1998) also deal with the geotechnical applications of the pulse test, particularly in connection with the performance of monitoring wells. SELVADURAI and CARNAFFAN (1997) successfully utilized the pulse test to determine the permeability characteristics of a cement grout used to seal fractures in geological materials. In the theoretical evaluation of the results for the pressure decay obtained from pulse tests, several additional material parameters need to be specified; these include the compressibility characteristics of both the unsaturated porous medium and that of the migrating fluid, the viscosity of the fluid and the porosity of the medium. These parameters must be obtained from supplemental experiments.

This paper discusses theoretical developments associated with the interpretation of the pulse test data by appeal to the decay of pressure in a fluid–filled borehole located in a porous medium of infinite extent. The radial flow option is considered to be a simpler alternative to the test involving one-dimensional rectilinear flow pulse tests. With one-dimensional tests, large pressures (large in relation to the pressures needed to initiate flow) must be applied to the cylindrical surface of the sample to maintain purely axial flow through the sample as opposed to an interface. This jacketing pressure could influence the alteration of the pore structure of the material leading to stress-dependent estimates of the permeability of the specimen. The results presented by TRIMMER *et al.* (1980) for tests conducted on Westerly granite indicate that permeabilities of the order of $10^{-24}$ m$^2$ can be observed when the confining net pressure is about 30 MPa. This is substantially lower than the value of $4 \times 10^{-19}$ m$^2$ applicable to Westerly granite tested in a virtually unstressed condition. The theoretical developments presented in the paper provide a basis for the use of conventional solutions for the pulse tests conducted in a borehole located in a porous medium of infinite extent, for the interpretation of tests conducted in a cylinder with

a co-axial cavity. The paper also discusses the development of an experimental facility and procedures for conducting pulse tests on relatively large specimens, measuring 457 mm in diameter, 510 mm in height containing a co-axial cylindrical cavity of diameter 51 mm. Finally, these developments are used to evaluate the permeability characteristics of an intact granite using results of pulse tests conducted on dry granite, saturated granite and saturated granite subjected to a heating-cooling sequence.

## 2. Theoretical Concepts

We consider the problem of the transient radial flow from a pressurized cylindrical cavity located in a *saturated* porous medium of infinite extent. The flow of water through the pore structure is assumed to be governed by Darcy's law and the pore fluid is assumed to be *compressible*. It is also assumed that the porosity of the medium is influenced only by the bulk compressibility of the medium. The *solid material* composing the porous medium is assumed to be *incompressible* in comparison with the pore fluid and the skeleton of the porous solid. Considering the equations of mass conservation and Darcy's law, it can be shown (see, e.g., FREEZE and CHERRY, 1979; PHILIPS, 1991; SELVADURAI, 2000) that the partial differential equation governing the transient variation of head $h(r,t)$ (units L) in the porous region is given by

$$\nabla^2 h = \frac{S}{T_R}\frac{\partial h}{\partial t}, \tag{1}$$

where

$$\nabla^2 = \frac{\partial^2}{\partial r^2} + \frac{1}{r}\frac{\partial}{\partial r} \tag{2}$$

is Laplace's operator referred to the radially symmetric coordinate system. In (1), $S$ is the storage coefficient of the tested interval $l$ (units L) (i.e.) the height of the specimen) defined by

$$S = l\gamma_w(nC_w + C_{\text{eff}}); \quad \text{(non-dimensional)}, \tag{3}$$

where $\gamma_w$ is the weight of water per unit volume (units $M/L^2\,T^2$; where M has units of mass and T has units of Temperature); $C_w$ is the compressibility of water (units $LT^2/M$); $C_{\text{eff}}$ is the compressibility of the porous skeleton (units $LT^2/M$); $n$ is the porosity (non-dimensional). Also, $T_R$, is the transmissivity of the tested interval (units $L^2/T$), which is related to $k_i$, the *hydraulic conductivity* (units L/T), of the *intact porous medium* by the relationship

$$T_R = k_i l = \frac{K_i l \gamma_w}{\mu}; \quad \text{(units } L^2/T), \tag{4}$$

where $K_i$ is the *permeability* of the intact porous medium (units $L^2$); $\mu$ is the dynamic viscosity of water (units M/LT). Equation (1), which is also referred to as the *elastic drive equation*, is an approximation to the generalized situation involving full coupling between the elastic deformations of both the porous rock fabric and the compressibility of the pore fluid (see, e.g., BIOT, 1941; MCNAMEE and GIBSON, 1960; RICE and CLEARY, 1976). In (1), the deformability of the fabric (or the skeleton) of the porous rock is introduced only through considerations of the *bulk volume change* properties of the porous fabric itself. An alternative to this approach is to assume that the porous fabric is perfectly rigid, in which case $C_{\text{eff}}$ is set equal to zero. It should also be noted that if $C_{\text{eff}}$ is zero and the fluid itself is incompressible, the storativity of the porous medium is zero and the transient effects in the flow process disappear; only a steady–state condition can exist. In this study both compressibilities are assumed to be finite.

For the experiments involving the large diameter granite cylinders, we examine the problem of radial flow from the pressurized central cavity for which the governing initial condition and boundary conditions are simplified as follows:

$$h(r,0) = 0; \quad a < r \leq \infty, \tag{5}$$

$$h(\infty,t) = 0, \tag{6}$$

$$h(a,t) = H(t), \tag{7}$$

$$H(0) = H_0, \tag{8}$$

where $a$ is the radius of the cavity. The initial condition (5) implies that at the start of the experiment the head distribution in the sample is uniform and defined to be zero. The boundary condition (6) implies that the outer boundary of the sample is remotely located from the inner boundary and that the head at that boundary is maintained at zero at all times. The boundary conditions (7) and (8) indicate that the head within the cavity is a time-dependent variable and has a constant value at $t = 0$. In addition to the conditions (5) to (8), a condition should be specified which states that the rate at which water flows from the cavity into the cylinder, as expressed by Darcy's Law applied to the inner cavity, is equal to the rate at which the water stored within the pressurized cavity expands as the pressure within it declines, i.e.,

$$2\pi a T_R \left[\frac{\partial h}{\partial r}\right]_{r=a} = V_w C_w \gamma_w \frac{\partial h}{\partial t}. \tag{9}$$

In (9), $V_w$ is the volume of water (units $L^3$) within the pressurized section of the system, which, in general, will include the volume of water in the entire pressurized length $l$, supply lines and other devices. [In the current experiments, the volume of the water in the leads and connections was less than one percent of the volume of water within the pressurized cavity.] It should be noted that the boundary condition (6) is an approximation for a cylinder with a finite outer radius. This assumption,

however, considerably simplifies the mathematical analysis of the initial boundary value problem governed by the partial differential equation (1).

The solution of (1), subject to the initial condition, boundary conditions and mass conservation criteria defined by (5) to (9), has been investigated in detail both in connection with unsteady state groundwater flow and the analogous problem in heat conduction (JACOB, 1940, 1947; CARSLAW and JAEGER, 1959; COOPER *et al.*, 1967; PAPADOPULOS *et al.*, 1973; BREDEHOEFT and PAPADOPULOS, 1980; HODGKINSON and BARKER, 1985; RUTQUIST, 1995; REHBINDER, 1996a,b). Only the result which pertains to the decay of head within the pressurized cavity is recorded here, and this can be expressed in the form

$$\frac{H(t)}{H_0} = \frac{P(t)}{P_0} = F(\alpha, \beta), \tag{10}$$

where $P(t)$ is the cavity pressure at time $t$ and $P_0$ is the cavity pressure at the start of the experiment, and

$$\alpha = \frac{\pi a^2 S}{V_w C_w \gamma_w}; \quad \beta = \frac{\pi T_R t}{V_w C_w \gamma_w}. \tag{11}$$

The function $F(\alpha, \beta)$ can be expressed in the integral form

$$F(\alpha, \beta) = \frac{8\alpha}{\pi^2} \int_0^\infty \frac{\exp(-\beta u^2/\alpha)}{u f(u, \alpha)} du, \tag{12}$$

where

$$f(u, \alpha) = [u\, J_0(u) - 2\alpha J_1(u)]^2 + [uY_0(u) - 2\alpha Y_1(u)]^2. \tag{13}$$

Also, $J_0(u)$ and $J_1(u)$ are, respectively, zeroth–order and first-order Bessel functions of the first kind and $Y_0(u)$ and $Y_1(u)$ are, respectively, zeroth– and first–order Bessel functions of the second kind (WATSON, 1944). Tabulated values of $F(\alpha, \beta)$ are given by COOPER *et al.* (1967), PAPADOPULOS *et al.* (1973) and BUTLER, Jr. (1998). For completeness, we also note that BREDEHOEFT and PAPADOPULOS (1980) have presented a useful approximation of the integral (12) in the form

$$F(\alpha, \beta) = e^{4\alpha\beta} erfc(2\sqrt{\alpha\beta}), \tag{14}$$

where *erfc* is the complementary error function, the tabulated values of which are given by ABRAMOWITZ and STEGUN (1964). BREDEHOEFT and PAPADOPULOS (1980) have shown that when $\alpha > 10$, the results (12) and (14) are virtually identical. For values of $\alpha$ less than 0.1, these authors have provided numerical values of $F(\alpha, \beta)$ which can be used for purposes of evaluating test data. These authors conclude that an error of two orders of magnitude in the estimation of $\alpha$ would result only in an error of less than 30% in the determined value of $T_R$.

To investigate the influence of the finite outer boundary on the result (10) we can develop the analogous result for the pressure transient problem where the boundary condition (6) is now replaced by the condition

$$h(b,t) = 0. \tag{15}$$

The resulting analysis is straightforward and various procedures and approximations for obtaining the solution are given by, among others, VAN EVERDINGEN and HURST (1949), COLLINS (1961) and BARENBLATT *et al.* (1990). The approach adopted here is slightly different although it essentially leads to the same conclusions, relating to the conditions of the test under which the finite outer boundary has no influence on the pressure decay rate within the pressurized cavity.

To perform the analysis we rewrite (1) in a non-dimensional form as follows:

$$\tilde{\nabla}^2\varphi = \alpha\frac{\partial\varphi}{\partial\beta}, \tag{16}$$

where

$$\tilde{\nabla}^2 = \frac{\partial^2}{\partial\rho^2} + \frac{1}{\rho}\frac{\partial}{\partial\rho}; \quad \rho = \frac{r}{a}; \quad \varphi = \frac{h}{H_0}. \tag{17}$$

By applying the Laplace transform with respect to $t$, defined by

$$\tilde{\varphi}(\rho,p) = \int_0^\infty e^{-p\beta}\varphi(\rho,\beta)d\beta, \tag{18}$$

where $p$ is the Laplace transform parameter, the general solution of $\bar{\varphi}(\rho,p)$ for the cylinder with a finite outer radius can be obtained in the form

$$\bar{\varphi}(\rho,p) = AK_0(\rho\sqrt{\alpha p}) + BI_0(\rho\sqrt{\alpha p}), \tag{19}$$

where

$$\begin{aligned} A &= \frac{I_0(\zeta\sqrt{\alpha p})}{\Delta}; \quad B = -\frac{K_0(\zeta\sqrt{\alpha p})}{\Delta} \\ \Delta &= I_0(\zeta\sqrt{\alpha p})\Delta_K - K_0(\zeta\sqrt{\alpha p})\Delta_I \\ \Delta_K &= 2\sqrt{\alpha p}K_1(\sqrt{\alpha p}) + pK_0(\sqrt{\alpha p}) \\ \Delta_I &= pI_0(\sqrt{\alpha p}) - 2\sqrt{\alpha p}I_1(\sqrt{\alpha p}) \\ \zeta &= \frac{b}{a} \end{aligned} \tag{20}$$

and $K_0$, $K_1$ and $I_0$, $I_1$ are modified Bessel functions of the first and second kind respectively, of order zero and unity (WATSON, 1944). It can be shown that the result (19) reduces to that given by COOPER *et al.* (1967) as $\zeta \to \infty$. It is possible to obtain an asymptotic solution of (19) which is valid for large $\zeta$. We note that

$$\frac{I_0(\zeta\sqrt{\alpha p})}{\Delta} \approx \frac{1}{\Delta_K}\left[1 + \pi^{2\zeta\sqrt{\alpha p}}\left(\frac{I_1}{\Delta_K}\right) + \cdots\right] \tag{21}$$

$$\frac{K_0(\zeta\sqrt{\alpha p})}{\Delta} \approx \frac{\pi e^{2\zeta\sqrt{\alpha p}}}{\Delta_K}[1 + \cdots]. \tag{22}$$

We now denote the result for $\zeta \to \infty$ by $\bar{\varphi}_\infty$. Consequently, we can show that

$$\bar{\varphi} - \bar{\varphi}_\infty = \pi e^{-2\zeta\sqrt{\alpha p}} \left[ \frac{\Delta_I K_0(\rho\sqrt{\alpha p}) - \Delta_K I_0(\rho\sqrt{\alpha p})}{(\Delta_K)^2} \right]. \tag{23}$$

The inverse Laplace transform of (23) is defined by

$$\varphi - \varphi_\infty = \frac{1}{2\pi i} \int_\Gamma e^{p\beta} (\bar{\varphi} - \bar{\varphi}_\infty)\, dp, \tag{24}$$

where $\Gamma$ is the BROMWICH contour for Laplace transform inversion. We set

$$I = \int_\Gamma e^{pt - 2\zeta\sqrt{\alpha p}} G(p, \rho)\, dp, \tag{25}$$

where

$$G(p, \rho) = \frac{\Delta_I K_0(\rho\sqrt{\alpha p}) - \Delta_K I_0(\rho\sqrt{\alpha p})}{(\Delta_K)^2}. \tag{26}$$

Evaluating $G(p, \rho)$ at $\rho = 1$, it can be shown that

$$G(p, 1) = \frac{2}{(\Delta_K)^2}. \tag{27}$$

Considering the asymptotic solutions of $\varphi(\rho,\beta)$, valid for large $\zeta$ and large $\beta$, it can be shown that

$$\left[\frac{H(t)}{H_0}\right]_{\zeta\to\infty} - \left[\frac{H(t)}{H_0}\right]_{\zeta\to\text{finite}} \approx \frac{4}{\sqrt{\pi\alpha\beta}} \frac{\exp[-\alpha(\zeta - 1)^2/\beta]}{[2 + (\zeta - 1)/\beta]} = \tilde{F}(\alpha, \beta, \zeta), \tag{28}$$

where $H(t)$ refers to the measured pressure head within the pressurized section. The result (28) can be used to estimate the range of applicability of the result (10) [or (14)] in terms of the aspect ratio $\zeta$, the non-dimensional time $\beta$ and the parameter $\alpha$.

It should be remarked that in all the theoretical developments presented here, it is implicitly assumed that the entire *accessible pore space* of the granitic rock is saturated with water. This makes Darcy's law admissible and the theoretical developments that will be used in the interpretation of the experimental results meaningful. If fluid migration during a pulse test is into an initially unsaturated or dry pore space (e.g., in the context of laboratory testing of recovered samples) the preceding theoretical developments are inadmissible. Under such circumstances, hydraulic pulse testing will involve the migration of a fluid front into the initially dry zone, and this represents a *moving boundary problem*. The solution of the moving boundary problem, including air displacement at the moving front, which in itself could be a fuzzy, non-distinct boundary, is a complex exercise and is certainly not the

most appropriate basis for an exercise in material parameter identification. In certain pulse tests conducted in connection with this research the granite cylinder is in a dry state, but it is likely that saturation of the cavity wall is induced prior to these tests, due to the initial pressurization of the cavity region. These tests are, however, considered to be important to the evaluation of the experimental data both qualitatively and quantitatively.

## 3. Experimental Facilities

The experimental facilities were developed as a part of a general research program related to the measurement of permeability of both intact and fractured samples of granite. The maximum external dimensions of the cylindrical samples used in the experimental investigations were 457 mm in diameter and 510 mm in height. To the authors' knowledge, these samples represent by far the largest that have been used in any laboratory experimentation involving measurement of permeability.

### 3.1 The Granite Cylinders

The granite used in the experimental research program was obtained from Barre, Vermont, U.S.A. Barre granite is a blue-gray granodiorite composed of approximately 23% quartz, 61% feldspars and 11% micas. Details of a petrographic analysis are given by HARDY (1991), who also presents the following values for the physical and mechanical properties: The average compressive strength determined from compression tests to failure (ASTM Standard C170-90) of samples measuring 55 mm in diameter and 110 mm in length was 205 MPa; the average flexural strength (ASTM Standard C880-89) of beam specimens measuring 300 mm in length, 38 mm in width and 25 mm in thickness was approximately 20 MPa; the average modulus of rupture (ASTM Standard C99-87) conducted on samples measuring 203 mm in length, 100 mm in width and 50 mm in thickness was approximately 17.7 MPa; the average bulk specific gravity (ASTM Standard C97-90) was 2.65 and the average water absorption (ASTM Standard C97-90) was 0.284%.

SELVADURAI (1996b,c) has investigated the thermo-physical properties of Barre granite in connection with a large–scale laboratory experiment that models the borehole emplacement concept proposed in nuclear waste disposal endeavors. The thermal conductivity ($\lambda$) of the granite is estimated at 2.5 J/m sec K and the heat capacity [$\rho_b\, C$; where $\rho_b$ is the bulk density (units $M/L^3$) and $C$ is the specific heat (units $L^2/KT^2$) ] is estimated at $2.38 \times 10^6$ J/m$^3$ K.

Altogether ***two*** granite cylinders were used in the experiments. These cylinders contained a central borehole measuring approximately 51 mm in diameter. The plane ends of the cylinders were polished to a mirror finish by the suppliers (Fig. 1). The

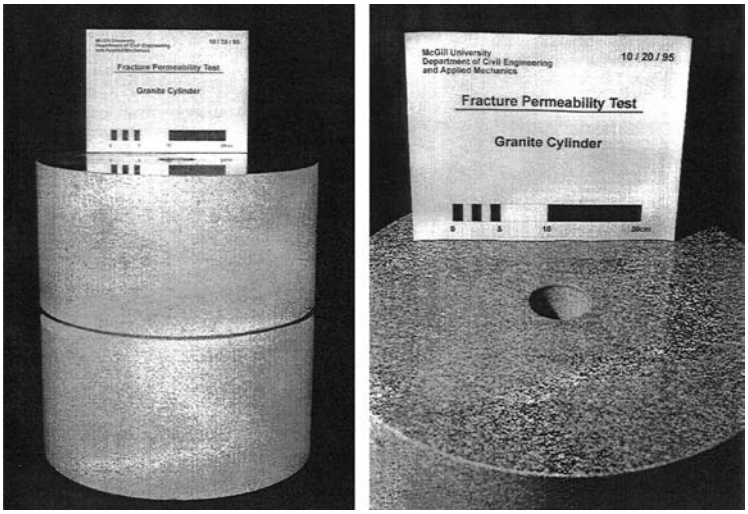


Figure 1
Hollow cylinders of Barre granite used in the experimental investigations.

cylindrical surfaces of the specimens were of a rough texture. The mid-plane of the specimens contained a V-notch shaped groove to a depth of 24 mm for purposes of initiating artificial fractures normal to the axis of the cylinder.

### *3.2 The Test Frame*

The test frame is a steel box structure where the base, the cross head and the uprights are made of highly stiffened welded sections. The upper cross-head of the frame accommodates the hydraulic jack used for application of the axial loads. The hydraulic jack is rated at a capacity of 1000 kips (4448 kN). The jack has a full stroke of 152 mm which allows for raising or lowering of the relatively heavy upper loading plate. The frame is designed to accommodate axial loads up to 4460 kN applied at the central axis. The loads applied to the hydraulic jack are transferred to the upper loading plate through a spherical seating rated to a load capacity of 4538 kN. The general arrangement of the test frame and the loading devices is shown in Fig. 2.

### *3.3 The Sealing Plates*

An adequate system for sealing the central fluid-filled cavity of the granite cylinders is essential to the success of pulse tests where the fluid in the cavity is subjected to high pressures. Separate stainless steel plates are provided at the plane ends of the cylinder to prevent corrosion of the loading plates. These stainless steel plates are 25 mm in thickness, have highly polished surfaces, and are also fitted with O-rings that provide a seal for the pressurization of the central cavity. The efficiency

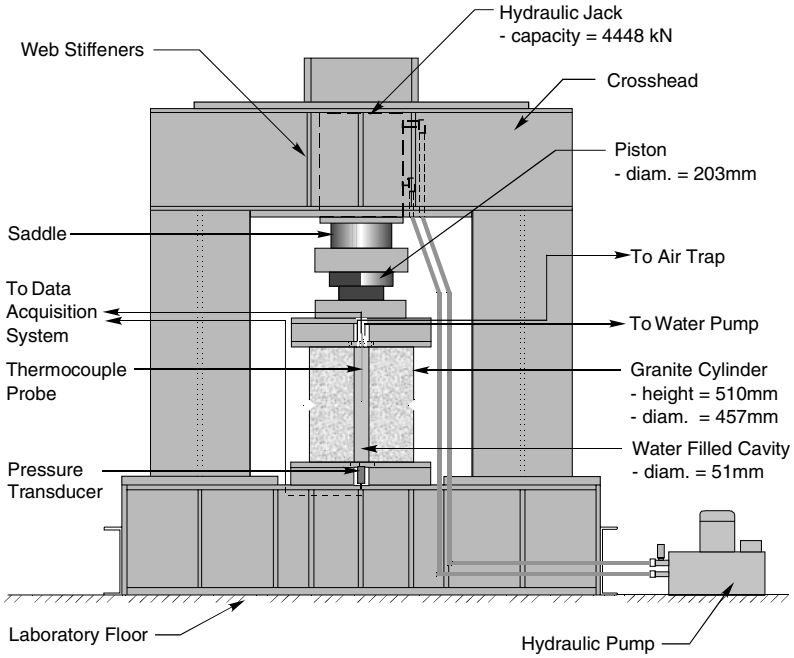


Figure 2
Schematic view of the experimental facility developed for conducting pulse tests on granite cylinders.

of sealing configurations of this type has been verified by the pressurization of hollow stainless steel cylinders over periods extending from 7 to 8 days. The stainless steel plates also contain specially designed couplings that are used to provide access to sensors and instrumentation within the water filled cavity. The stainless steel plate at the base of the sample is incorporated with a pressure transducer (maximum pressure capacity 2070 kPa) to measure fluid pressures within the cylindrical cavity during pulse tests. The upper stainless steel plate contains a specially designed coupling unit that provides access for the inlet and outlet ports for water supply. A thermocouple probe (temperature range –200 °C to 900 °C) is used to measure the temperature of the water in the cavity during a test. All inlet and outlet leads for water supply are made of stainless steel and Swagelok valves (maximum pressure rating of 20.7 MPa) are used to seal the fluid pressure in the cavity during a pulse test.

### *3.4 The Water Supply System*

For safety reasons, the maximum pressures applied to the internal cavity were substantially lower than the tensile strength of the granite as determined from diametral compression tests. An additional limiting factor pertained to the efficiency

of the seals. The analysis conducted by SELVADURAI and CARNAFFAN (1997) for experiments involving grout samples also indicates that for the experimental configuration involving radial flow with pressures up to 1 MPa, the corrections to the theoretical basis for the pulse test necessary to account for elastic expansion of the cylinder induced by the internal pressure are negligible. The volumetric fluid pump used as the water supply unit had a pressure range of 1 MPa to 8 MPa at fluid flow rates ranging from 0.10 ml/min to 150 ml/min.

### *3.5 The Data Acquisition*

The sensors to be monitored in an experiment included the pressure transducer at the base plate, which monitors the time-dependent variations in pressure in the central cavity; a pressure transducer, which monitors hydraulic pressure in the load cell used to apply axial loads; and the thermocouples, which measure the temperatures both within the central cavity and at the outer surface of the cylinder.

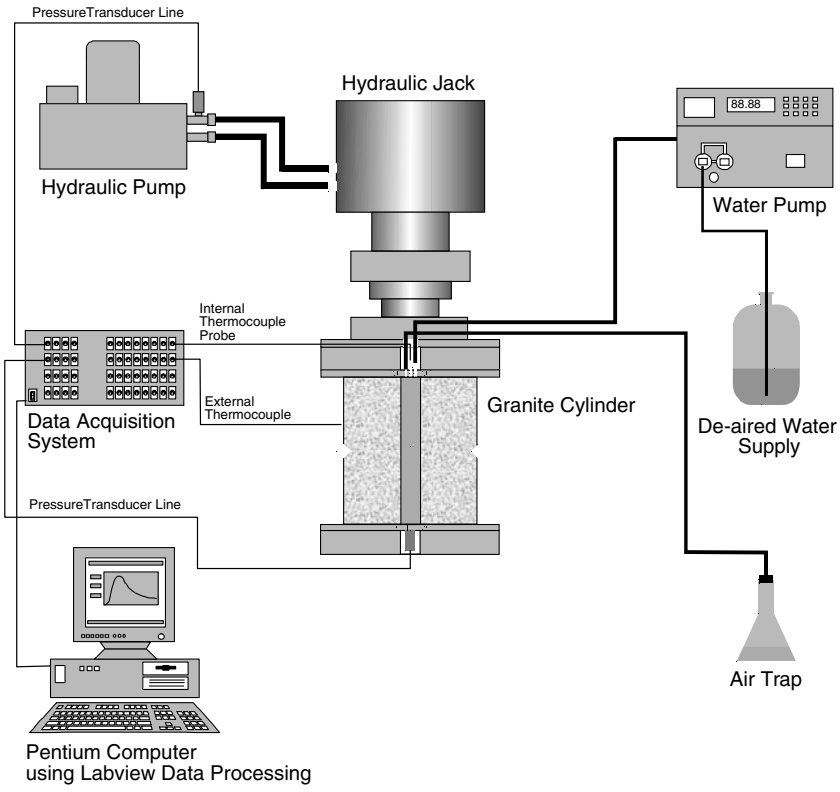


Figure 3
Schematic view of the experimental configuration for conducting pulse tests on granite cylinders.

The cavity pressure transducer needed to be monitored continually to observe accurately the time-dependent decay of the fluid pressure. During each experiment, all data were acquired and stored; the software was configured to give real time displays of critical responses in an experiment (e.g., time-dependent decay of the pressure within the central cavity). The schematic arrangements of the test facility, the layout of the water supply system, the loading devices, the sensors and the data acquisition system are shown in Fig. 3.

## *4. Experimental Procedures*

A set of consistent procedures was adopted for conducting pulse tests on the intact granite cylinders that were either in an air-dry, as-supplied condition, or heated in an unsaturated condition, or saturated by long–term water flow at a constant flow rate, or subjected to a heating sequence after a period of saturation. In addition to the pulse tests, several ancillary tests were conducted to determine the physical and mechanical properties of the granite.

### *4.1 Sample Assembly Procedure for Pulse Tests*

The pressure transducer was first attached to the 25 mm stainless steel plate A containing an inset groove for an O-ring seal, and the center of the plate positioned to coincide with the final position of the axis of the sample. A 6 mm thick Neoprene sheet, 500 mm square was placed on the surface of the plate A and a circular cut-out is made in this sheet to expose the O-ring seal. The Neoprene sheet ensures nearly uniform contact stresses between the base plate and the cylindrical sample. (In certain experiments that did not incorporate this layer, localized contact between the loading plates and the granite cylinder lead to either splitting failure of the sample or damage to the highly polished granite surface, which resulted in fluid leakage from the sealing surfaces.) The granite cylinder was then placed on the Neoprene sheet making sure that the cylindrical cavity was directly above the pressure transducer at the base plate A. The seal for the upper surface was achieved in the same manner but by using a spray adhesive to keep the O-ring and the Neoprene sheet attached to the upper stainless steel plate B of thickness 15 mm. This upper plate was also equipped with a Swagelock Quick Connector adaptor, a thermocouple adaptor and a welded stainless steel tube, which was used for de-airing the fluid–filled cavity. A thermocouple probe was also attached to the adaptor. These leads emerge through a slot in a 25 mm thick plate, which serves to protect the leads and connections during application of the axial loads. The final loading housing containing the spherical seating is placed over a 600 mm square, 75 mm thick steel plate and the piston jack is lowered to the loading plates without imposing any loads.

All instrumentation is connected to the data acquisition system and the air outlet attached to a glass reservoir.

### *4.2 Procedure for Pulse Tests*

Since pulse tests by themselves are not standardized tests, several aspects of the testing sequence had to be specified in order to establish some consistency in the methods of testing. First, using the hydraulic jack system, the granite cylinder was subjected to an axial stress, which varied between 2200 kPa and 2400 kPa. Since the axial stress induced by the self-weight of the loading plates was relatively small (25 kPa) this additional stress was necessary to compress the O-ring and the Neoprene sheet and to generate the necessary sealing. The central cavity was filled with de-aired water until excess water emerged from the air outlet. The outlet valve was then closed and the water supply pump set to a maximum flow rate of 100 ml/min, and to a maximum pressure of 1800 kPa. This procedure was repeated several times upon attainment of the set flow rate. The air outlet valve was opened to release any air bubbles trapped in the water-filled cavity and the axial stress is re-set to 5000 kPa. In tests involving granite cylinders in their as-supplied condition, the cavity is further subjected to a cavity fluid pressure of 1800 kPa for one hour prior to each pulse test. The purpose of this priming pressure is to prevent the release of air from the dry sample to the fluid in the central cavity. The presence of air would have the overall effect of altering the effective compressibility of the water in the cavity region, which could unduly influence the interpretation of the test results. When conducting each pulse test, this procedure was repeated and in each test the *starting pressure was set to* 600 kPa. There is the question as to whether the application of the axial stress can lead to pore pressure generation in the cylinder that would result in an initial condition different to that defined by (5). Similar comments can be made with regard to the initial cavity pressure applied to prime the system in preparation for the pulse tests. There are no direct means of assessing the influence of any initial pore pressure distributions. With regard to the pore pressures that could be generated at the interior of the cylinder, their dissipation is accommodated for by prolonged periods (approximately 12 to 24 hours) between tests.

In tests involving saturation of the granite cylinders, the internal cavity was subjected to a flow rate of approximately 0.10 ml/min for a period of 144 hours. Although the flow rate was steady, the pressure within the cavity did exhibit fluctuations until a steady–state pressure range (between 800 kPa and 1000 kPa) was observed. This near constant flow rate was maintained for a further 144 hours until there was evidence of water migration to the boundary of the cylinder through a visible "sweating discoloration" of its outer cylindrical surface. The discoloration was initially non-uniform; with time, however, the surface exhibited signs of uniform saturation. A mass balance calculation indicates that this duration of the fluid supply at the specified rate was sufficient to saturate the accessible void space consistent with

the porosity of the granite of 0.011 (i.e., volume of the void space is $9.2 \times 10^{-4}$ m$^3$ and the volume of fluid supplied after 288 hours is $17.28 \times 10^{-4}$ m$^3$. From this calculation we can only make the plausible assumption that the accessible void space was completely saturated). Upon completion of this saturation phase, the fluid pressure was allowed to dissipate in a transient fashion. Before formal pulse testing commenced on the saturated samples, the axial stress on the cylinder was adjusted to 5000 kPa. The cavity was then pressurized to 600 kPa and the pressure maintained for 5 minutes to stabilize the data acquisition. The air outlet valves were opened to release any air that may have accumulated within the cavity. The valves were then closed and the pump re-activated. As the pressure within the central cavity approached 600 kPa, the flow rate was reduced to 0.10 ml/min and the water inlet valve was closed when the data acquisition system indicated a cavity pressure of 600 kPa. The decay of the water pressure in the cavity was recorded every 2 seconds and the experiment terminated when the pressure reduced to 170 kPa. This procedure was repeated in all experiments involving pulse tests, excluding those that were tested from a dry, as-supplied condition. Approximately 12 to 24 hours elapsed between each pulse test.

### *4.3 Heating of Granite Cylinders*

The motivation for conducting pulse tests on granite cylinders that are subjected to heating stems from the need to assess the influence of heating on the permeability characteristics of the granite. Thermal expansion of dry granite can induce microstructural alterations at grain boundaries, which could change the permeability of the granite. With saturated granite, the differential thermal expansion between the pore fluid and the porous matrix is visualized as an effect that can contribute to microcracking at the grain level, thus leading to changes in the permeability. Pulse tests on the heated granite were carried out primarily as a preliminary investigation to assess the degree of alteration in the permeability of the granite when subjected to the range of temperatures ($< 100$ °C) of interest to the research program. The objective of this phase of the research was to uniformly heat the granite cylinder to a prescribed temperature in either a dry state or a completely saturated state. This is ideally achieved by uniformly heating all the exposed surfaces of the cylinder to the same temperature. The size of the cylinder precludes this option. The only possible alternative was to apply heating to the cylinder in its final assembled configuration for pulse testing. This restricted heating only to the exterior cylindrical surface. Although some precautions can be taken to minimize the non-uniformity in the temperature distributions within the cylinder, these cannot be avoided altogether.

With a few exceptions, the sample assembly procedure largely followed that described in Section 4.1. The Neoprene sheets were replaced by thin ceramic wool layers to insulate the plane ends of the cylinder (Fig. 4). Three pairs of sequential semi-circular band heaters, with heater elements each having an output of 300 Watts, were placed on the outer surface of the granite cylinder. The heater bands were connected to a voltage

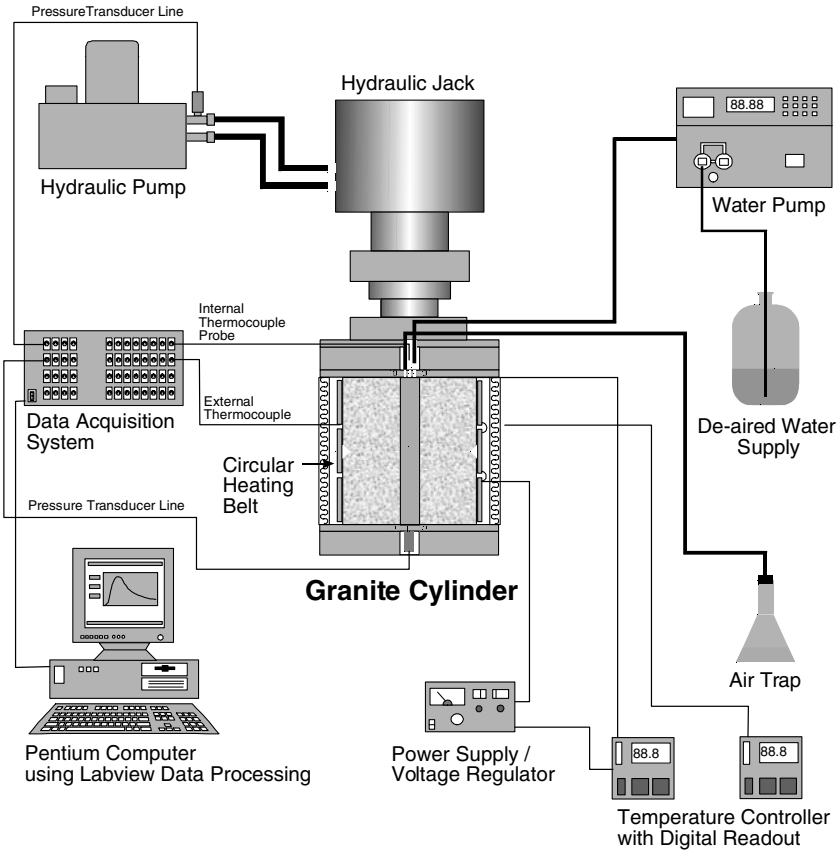


Figure 4
Schematic view of the experimental configuration for conducting pulse tests on externally pre-heated and cooled granite cylinders.

regulator and a thermocouple conditioner equipped with a digital readout. The thermocouple was placed on the plane end of the granite cylinder midway between the cavity and the outer boundary. The entire cylindrical surface was insulated with three layers of an air pocket/aluminum foil sandwich sheet with a total thermal resistance of 22 RSI. In one heating arrangement, the granite cylinder was heated only through these external heaters and the inner cavity was kept filled with water. When the average temperature in the water and at the controlling thermocouple located on the upper plane surface reached 90 °C, the heating was terminated and the granite cylinder was allowed to cool down to the ambient temperature of 23 °C. Here again, the cavity pressure was increased to 1800 kPa for 1 hour prior to conducting pulse tests, at a starting cavity pressure of 600 kPa. In certain experiments, the granite cylinder in its dry, as-supplied condition was subjected to a temperature of 90 °C and allowed to cool

to the ambient temperature of 23 °C. A granite cylinder that had been subjected to prolonged saturation was also subjected to exterior heating with the central cavity sealed and filled with water. In the saturated condition the temperature of the external surface of the granite was raised to 180 °C. The heating was terminated when the controlling thermocouple reached a temperature of 80 °C. The temperature of the water at the termination of the heating was approximately 105 °C. It is unrealistic to assume that the temperature of the entire granite cylinder was raised to the maximum recorded; a realistic average temperature in the granite would correspond to about 140 °C. Further details of this experiment are given by SELVADURAI (1997).

### *4.4 Mechanical and Physical Properties of the Granite*

In addition to the permeability tests, separate laboratory tests were performed to determine the elastic constants [Young's modulus ($E$), Poisson's ratio ($v$), porosity ($n$) and the coefficient of thermal expansion ($\alpha_0$)] of the granite. The elastic parameters of the granite were determined from uniaxial compression tests on cylindrical samples of the granite measuring 105 mm in diameter and 203 mm in height. In their as-supplied condition, the plane ends of these cylindrical samples were smooth and parallel. The tests were conducted using a servo-controlled MTS testing machine especially designed for testing concrete and other high strength brittle materials. The granite cylinder was fitted with axial and circumferential extensometers to determine, respectively, the axial compression and the diametral expansion of the cylinder. The procedure adopted in performing these tests corresponds to the ASTM standards applicable to such tests (ASTM C 469, 1994). The samples were tested at a loading rate of 227 kPa/sec. The experiments yielded the following estimates for the elastic constants: Young's Modulus ($E$) = 60 GPa; Poisson's Ratio ($v$) = 0.13. Compressive and tensile strength tests carried out on specimens of the granite gave the following results: compressive strength

Table 1

*Mechanical and physical properties of the Barre granite*

| Property | Estimate | Reference |
|---|---|---|
| Porosity ($n$) | 0.011 | Core Laboratories Report |
| Bulk Density ($\rho_b$) | 2630 kg/m$^3$ | Core Laboratories Report |
| Grain Density ($\rho_g$) | 2660 kg/m$^3$ | Core Laboratories Report |
| Maximum Air Permeability ($K_a$) | 3 x $10^{-17}$ m$^2$ | Core Laboratories Report |
| Coeffcient of Linear Expansion ($\alpha_0$) | (8.1 to 10.2) $\times$ $10^{-6}$/°C | This Research Programme |
| Thermal Conductivity ($\lambda$) | 2.5 J/msec°K | SELVADURAI (1996b,c) |
| Heat Capacity ($\rho_b C$) | 2.38 $\times$ $10^6$ J/m$^3$°K | SELVADURAI (1996b,c) |
| Young's Modulus ($E$) | 60 GPa | This Research Programme |
| Poisson's Ratio ($v$) | 0.13 | This Research Programme |
| Tensile Strength ($f_t$) | 9.00 MPa | This Research Programme |
| Comp. Strength ($f_c$) | 126 MPa | This Research Programme |

$f_c = 126$ MPa; tensile strength $f_t = 9$ MPa. These values are in general agreement with the results obtained by HARDY (1991) for the mechanical properties of Barre granite. The coefficient of thermal expansion of the granite was determined by heating an unconstrained sample to a specified temperature. The estimates for the coefficient of linear expansion ranged between $8.1 \times 10^{-6}$/ °C and $10.2 \times 10^{-6}$/ °C.

The porosity of Barre granite was determined at the Core Laboratories in Calgary, Alberta, using the "Analytical Procedures" proposed in the *American Petroleum Institute* (1960) guidelines, although the tests were performed on only one cylindrical sample of the Barre granite. The experimental evaluations conducted by Core Laboratories included the measurement of the bulk density, the grain density and the maximum air permeability. The results obtained from the tests were as follows: Porosity = 0.011; Dry Density = 2630 kg/m$^3$; Grain Density = 2660 kg/m$^3$; Maximum Air Permeability = 0.03 md $\cong 3 \times 10^{-17}$ m$^2$. The mechanical and physical properties of Barre granite are summarized in Table 1.

## 5. Experimental Results

Prior to the presentation of the experimental results it is useful to demonstrate that for typical low permeability materials (e.g., $K_i$ in the range $10^{-17}$ m$^2$ to $10^{-22}$ m$^2$) the analytical result developed for the decay of pressure in a cavity located in a porous medium of *infinite extent* can be used to estimate the permeabilities from the short duration pulse tests. Considering the experimental configuration of the granite cylinder and the physical properties of water, we have

$$2a = 0.051 \text{ m}; \quad 2b = 0.457 \text{ m}; \quad L = 0.510 \text{ m}. \tag{29}$$

Hence

$$\beta = \frac{\pi K_i L t}{V_w C_w \mu} \cong \frac{K_i t}{a^2 C_w \mu}. \tag{30}$$

For

$$\begin{aligned} a^2 &\cong 6.5 \times 10^{-4} \text{ m}^2; \qquad C_w \cong 4.4 \times 10^{-7} \text{ m}^2/\text{kN}; \\ C_{\text{eff}} &\cong 3.75 \times 10^{-8} \text{ m}^2/\text{kN} \qquad \mu \cong 10^{-6} \text{ kN} \cdot \text{sec}/\text{m}^2 \end{aligned} \tag{31}$$

we have $\beta \cong 3.5 \times 10^{15} K_i t$, where, for consistency, $K_i$ is expressed in m$^2$ and $t$ is expressed in seconds. For the range of permeabilities that could be encountered for materials such as granite [i.e., $K_i \in (10^{-17}$ m$^2$, $10^{-21}$ m$^2)$ and for the duration of the test $t \cong 2100$ seconds, we have $\beta \in 7.35 \times (10, 10^{-3})$. For the experimental configuration and for the granite used in the investigation

$$\alpha = \frac{\pi a^2 S}{V_w C_w \gamma_w} \cong \left(n + \frac{C_{\text{eff}}}{C_w}\right) \cong 0.10; \quad \zeta = \frac{b}{a} \cong 9. \tag{32}$$

Thus, evaluating (28) we have

(i) for $\beta = 7.35 \times 10$; $\tilde{F}(\alpha, \beta, \zeta) \cong 1.0 \times 10^{-2}$

(ii) for $\beta = 7.35 \times 10^{-3}$; $\tilde{F}(\alpha, \beta, \zeta) \to 0$.

It is clear that the exponential term in (28) is dominant and appreciable differences between the result for the cavity in an infinite medium and the cavity located in a cylinder of finite outer radius will manifest only if $(\alpha(\zeta-1)^2/\beta) \ll 1$. Therefore, with the given experimental configuration involving the low permeability granite, the solution of the pressure decay in a cavity located in a saturated porous medium of infinite extent could be used to estimate the permeability of the granite, provided the duration of the pressure decay used in the estimation procedure does not exceed $10^4$ seconds. [This observation can also be supplemented by considering the results originally given by VAN EVERDINGEN and HURST (1949) and also cited by COLLINS (1961); from the results given by the latter (page 121), it would appear that for a radii ratio of $\zeta = 9$, the solution for the problem involving the *finite outer boundary* diverges from the solution applicable to the *infinite outer boundary* when $t_D = \beta/\alpha \approx 30$. Considering the values for $\beta = 3.5 \times 10^{15}\, K_i t$; $\alpha = 0.10$ and restricting the permeability to $K_i \approx 10^{-19}$ m$^2$, it is evident that the solution for the problem involving an infinite domain can be used as a satisfactory solution for a domain with $\zeta = 9$,

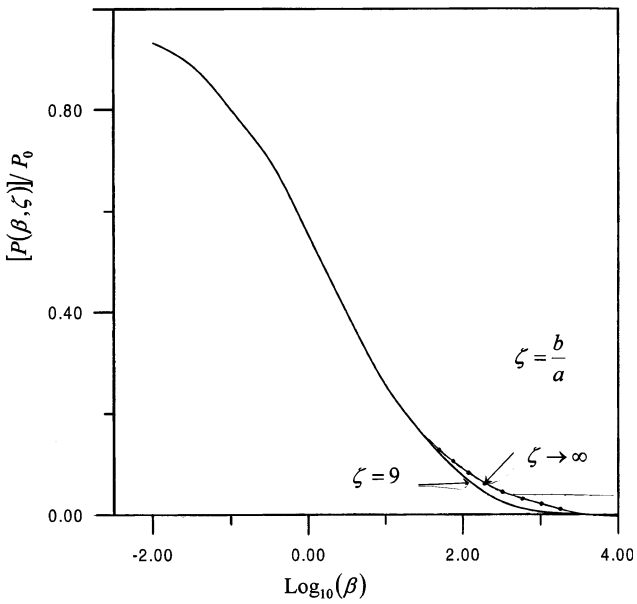


Figure 5
Time-dependent decay of cavity pressure: influence of the external boundary.

provided $t < 10^4$ seconds. This analysis does provide an independent confirmation of the result that is used quite extensively in the literature.] Fig. 5 illustrates the comparison between the time-dependent decay of pressure within the cavity for the two cases involving the porous medium of infinite extent and for a cylinder with a finite outer radius ($\zeta = 9$). The simpler result (10) for the cavity located in an infinite medium will thus be used for the purposes of estimation of the permeability of the granite tested under various conditions.

### *5.1 Pulse Tests on Unsaturated Granite*

Pulse tests were first conducted on the granite cylinder in its *unsaturated* condition and at room temperature (23 °C). Altogether, 6 pulse tests were performed [Test Set 1]. The results for the pressure decay in the central cavity region obtained from these tests are shown in Fig. 6. The theoretical estimates for the pressure decay curves derived from the result (10) are also shown in Fig. 6. It should be noted that in the presentation of the comparisons, the permeability of the granite is estimated as a *range of values* determined from the theoretical evaluations. No attempt is made to derive an explicit value for the permeability by adopting either least–squares or other

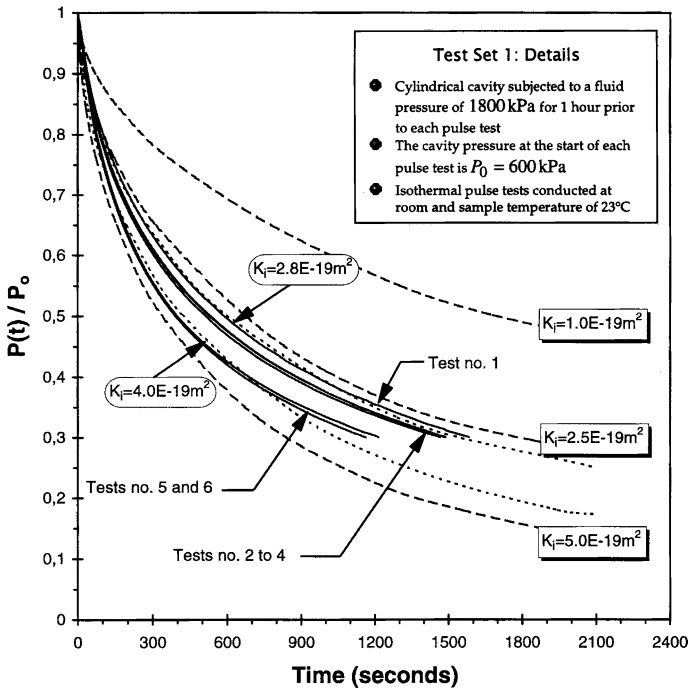


Figure 6
Pulse tests on unsaturated granite.

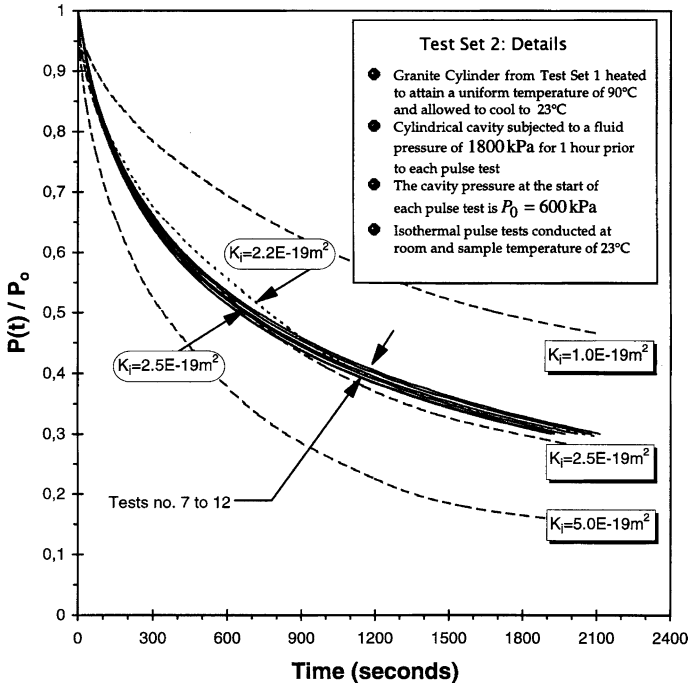


Figure 7
Pulse tests on unsaturated granite subjected to a heating-cooling cycle.

curve-fitting techniques. The estimated values for the permeability, $K_i$, for Barre granite (in its *as-supplied* condition) derived from these tests range between (2.8 to 4.0) $\times 10^{-19}$ m$^2$. In a further test, the granite cylinder, in its condition at the termination of the first set of pulse tests, was subjected to heating. When the temperature at the surface of the cylinder and within the fluid in the cavity reached 90 °C, the heating was terminated, and the sample allowed to cool down to the ambient temperature (23 °C). Altogether, 6 pulse tests were conducted on the pre-heated sample. The results for the pressure decay in the central cavity region obtained during these tests are presented in Fig. 7 [Test Set 2]. The theoretical estimates for the pressure decay in the cavity derived from the result (10) are also presented in Fig. 7. The estimated range of values for the permeability, $K_i$ of the granite derived from these tests is (2.2 to 2.5) $\times 10^{-19}$ m$^2$.

In a final series of tests involving the *as-supplied* granite, a new dry granite cylinder was subjected to heating to attain a nearly uniform temperature of 90°C. After this period, the heating was terminated and the sample allowed to reach thermal equilibrium with the ambient environment (23 °C). The pressure decay curves obtained from these tests are shown in Fig. 8 [Test Set 3]. The estimated range

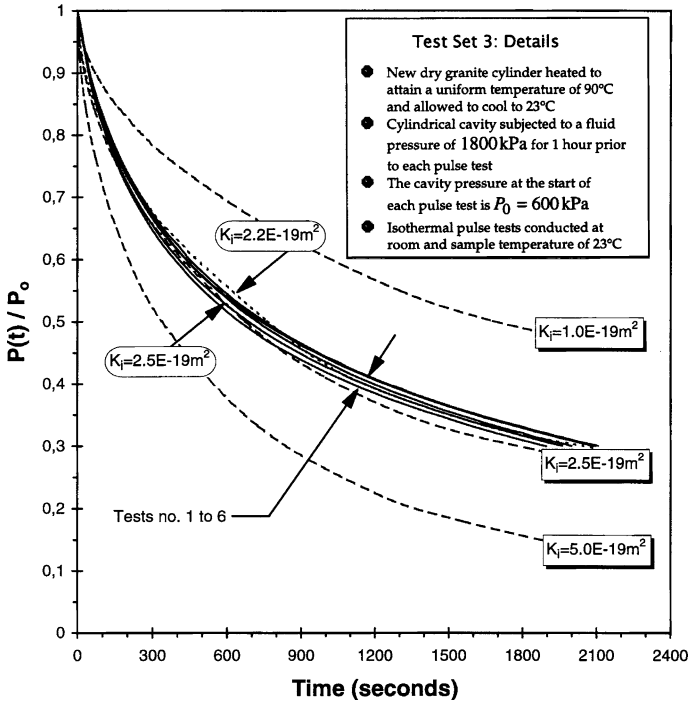


Figure. 8
Pulse tests on unsaturated granite subjected to a heating-cooling cycle.

of values for the permeability, $K_i$ of the granite derived from these six tests is (2.2 to 2.5) $\times 10^{-19}$ m$^2$.

### *5.2 Pulse Tests on Saturated Granite*

In these tests the central cavity of the granite cylinder was subjected to a constant flow rate of 0.1 ml/min. The outer surface of the granite specimen was kept uncovered throughout the saturation phase. Relatively uniform wetting discoloration of the outer surface was observed after 3 days of application of constant flow to the sample. Fig. 9 illustrates the typical time-dependent variation in the water pressure in the fluid-filled cavity during the application of a constant flow rate over a six-day period. This flow rate was maintained over a period of 12 days. Pulse tests were conducted on the saturated sample immediately following the constant flow rate saturation sequence. The time-dependent decay of the cavity pressure in the pulse test is shown in Fig. 10 [Test Set 4]. The estimates for the permeabilities determined from the six pulse tests range from (2.0 to 3.0) x $10^{-19}$m$^2$. Pulse tests were also conducted on the same sample after 1 day of a constant flow/saturation process. The results for

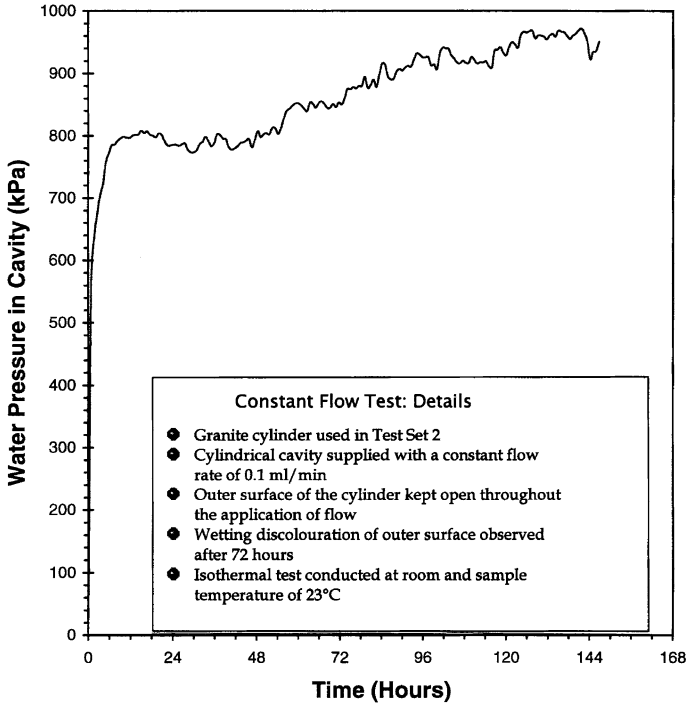


Figure 9
Time-dependent variation of fluid pressure in cavity during application of a constant flow rate.

the pulse test are shown in Fig. 11 [Test Set 5]. The estimate for the permeabilities determined from 6 tests vary from (1.6 to 2.3) $\times 10^{-19}$ m$^2$.

### *5.3 Pulse Tests on Granite Cylinder Subjected to Saturation and Heating*

In this test, the saturated granite cylinder was subjected to external heating, with the cavity of the granite cylinder filled with water. The *average* temperature in the granite cylinder was estimated at approximately 140 °C and the controlling thermocouple located at the upper plane surface of the cylinder reached 80 °C. A series of pressure pulse tests were conducted on the granite cylinder after sufficient time was allowed for it to cool to 26 °C with the ambient temperature maintained at 23 °C [Test Set 6]. The test results shown in Fig. 12 indicate permeability estimates that range from (3.0 to 3.8) $\times 10^{-19}$ m$^2$. It was anticipated that the residual heat in the cylinder might cause a minor increase in the water temperature and for this reason, in the interpretation of the results of these pulse tests, the value of the viscosity of the water has been adjusted to take into account the maximum

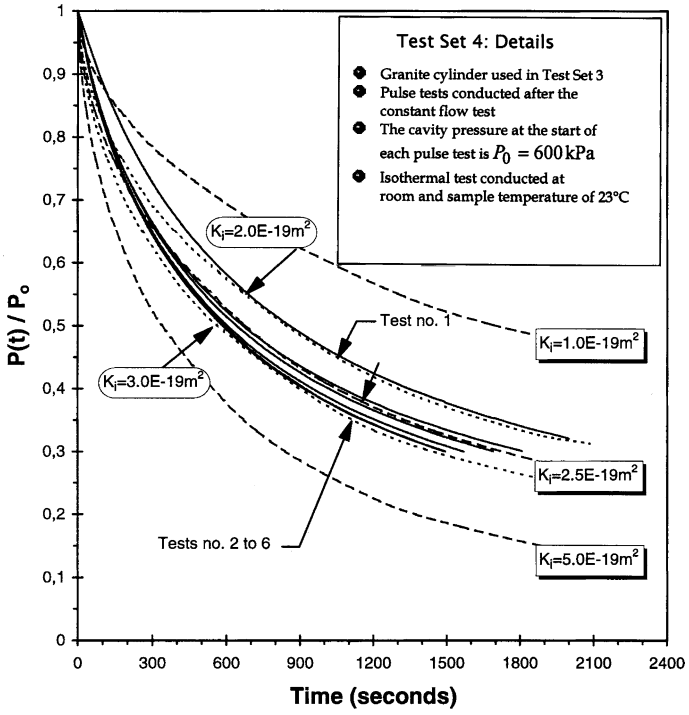


Figure 10
Pulse tests conducted on granite cylinders subjected to a constant flow rate.

temperature. Finally, this sample was subjected to a constant flow rate of 0.1 ml/min for 12 days. Again, relatively uniform discoloration of the surface of the sample was observed within 3 days. Figure 13 illustrates the time-dependent variation in fluid pressure, over a 6 day period, upon attainment of a *steady-threshold* peak in the cavity fluid pressure.

A final series of pulse tests was conducted on the granite cylinder in its condition after the saturation-heating-cooling-resaturation sequence [Test Set 7]. The Fig. 14 illustrates the time-dependent decay of pressure within the cavity. The permeability estimates range from (2.8 to 3.2) $\times 10^{-19}$ m$^2$. The results for permeability derived from all tests are summarized in Table 2.

## 6. Discussion and Conclusions

The intact permeability of low porosity crystalline geological materials such as granite is an important parameter to many geophysical and geoenvironmental applications. In the particular context of flow of fluids in *tight fractures* located in such geological media, the intact permeability of the matrix is expected to influence

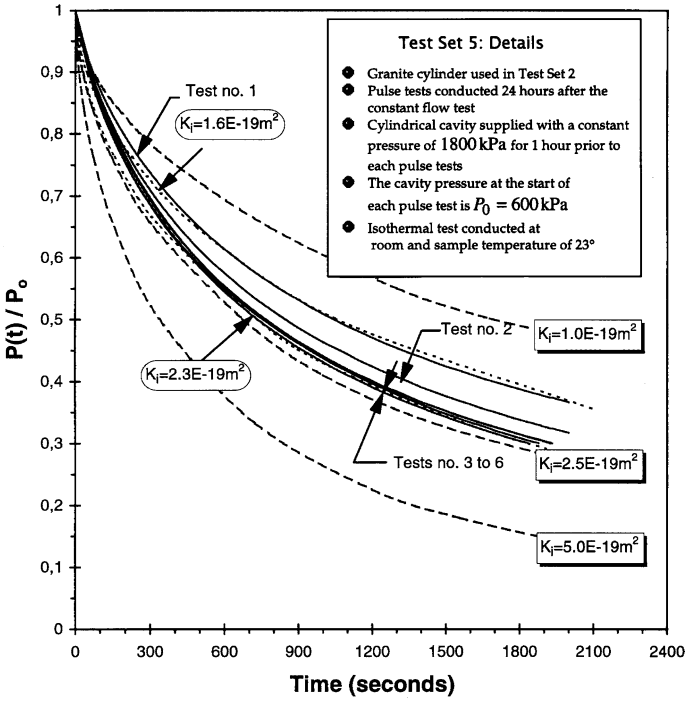


Figure 11
Pulse tests conducted on granite cylinders subjected to a constant flow rate.

the flow in both the fracture and the porous medium in general. Research investigations show that the radial flow-type pulse tests, used quite extensively for the *in situ* measurement of permeability, can be adapted quite conveniently to develop a laboratory-type radial flow configuration. The radial flow option, due to the self-equilibrating nature of the applied stresses, is perhaps an easier experimental configuration than tests involving one-dimensional rectilinear flow pulse tests. In both cases, however, sufficient pressures should be applied to generate the sealing effect. These stresses could have a secondary effect in altering the assumptions pertaining to the initial conditions (particularly due to possible excess pore pressure generation) applicable to the mathematical modelling and the interpretation of the test. In the current series of tests sufficient time was allowed between the preparation for the test and the performance of the pulse tests. Without a complete poroelastic analysis of the compressed granite cylinder, which in itself would require a knowledge of the permeability of the granite, it is not possible to clearly establish both the magnitude of the pore fluid pressures and their time-dependent decay. On the other hand, if such residual pore pressures were present, the decay responses for the pulse tests would exhibit a marked scatter, resulting from a cumulative (residual) effect that would persist in each pulse test. The repeatability of the results for all the

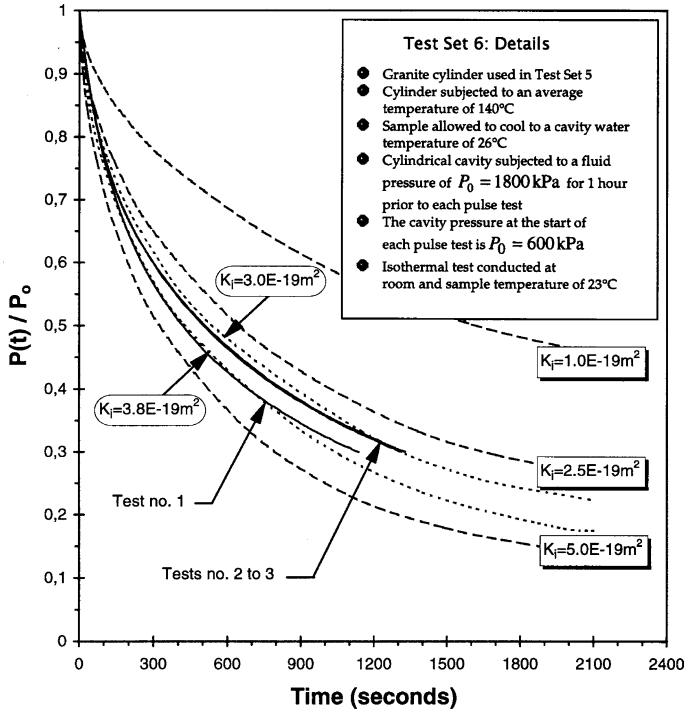


Figure 12
Pulse tests conducted on granite cylinders subjected to a constant flow rate.

pulse tests suggests that the initial condition applicable to each test is approximately the same, and this would point to the validity of the zero pore fluid pressure initial condition.

In this research we conducted permeability tests on granite specimens substantially larger than hitherto reported in the literature. The current tests belong on a *scale* intermediate between laboratory and field studies for situations involving low ambient stress fields. This research shows that, within certain limits, the classical solution for the pressure decay in a borehole located in a porous medium of infinite extent can be conveniently adopted to evaluate the pulse test data derived from a cylinder with a finite external radius. In the context of application of the results to deep geological repositories, the influence of the ambient stress field on the permeability characteristics is certainly an important consideration. It is equally important to determine the permeability in the unstressed state, which is particularly representative of conditions in certain locations of open, wide galleries in deep geological repositories.

The permeability of the intact granite is assessed under conditions of an *as-supplied* dry state, a full saturation state and the heating of the saturated granite

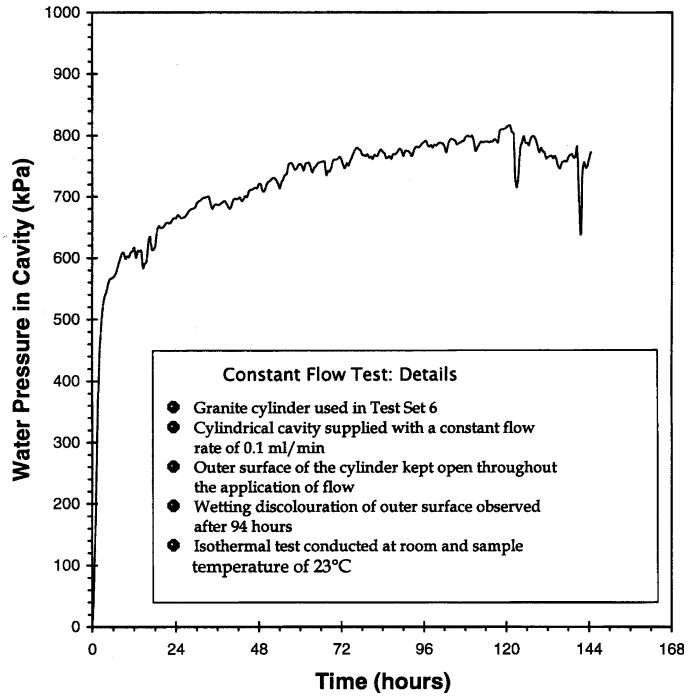


Figure 13
Time-dependent variation of fluid pressure in cavity during application of constant flow rate: granite subjected to a heating-cooling cycle.

cylinder to an average temperature of approximately 140 °C. An important feature of these experiments is the ability to obtain reasonably repeatable results for a given set of experimental conditions. It is observed that the tests carried out on "*air dry*" or "*unsaturated*" samples subjected to moisture influx in a pulse test give a wide variability within the set of tests. It should therefore be remarked that the permeability derived from pulse tests on "unsaturated" granite cylinders can be interpreted only as an "*apparent permeability*" for the unsaturated granite. The saturation of the granite prior to pulse testing provides experimental data closely indicative of the intact permeability of the granite. The heating of the saturated granite to an average value of approximately 140 °C does not result in a marked change in the short-term permeability estimates for the granite. The range of temperatures under which these tests were carried out was guided by the objectives of the research program; it is quite feasible to assume that application of higher temperatures could result in the pore fluid having a greater influence on the internal fabric of the granite due to the generation of excess fluid pressures; this in turn could lead to higher estimates of permeability. The experimental configuration does not lend itself to maintaining a constant uniform temperature field throughout the

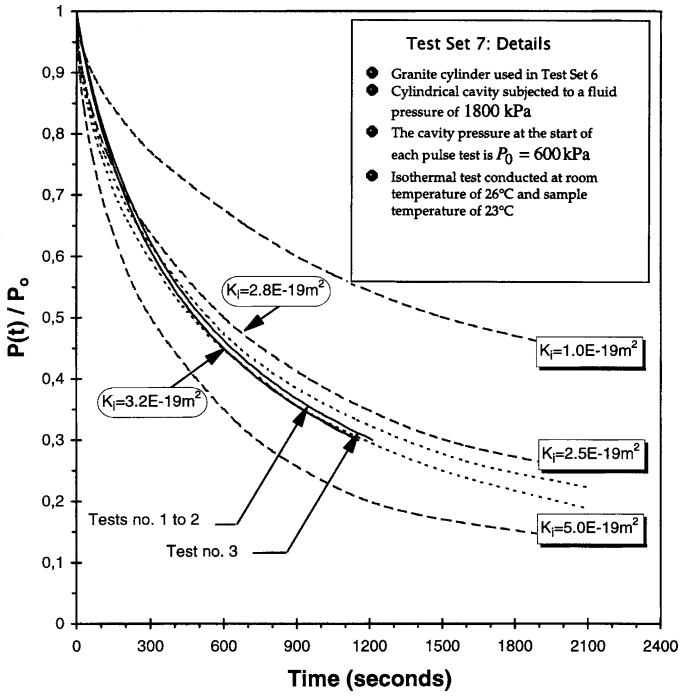


Figure 14
Pulse tests conducted on granite cylinders subjected to heating-cooling cycle followed by fluid supply at a constant flow rate.

sample. The interior temperatures in the cylinder can be inferred only through calculations; the absence of thermocouple installations within the sample thickness is mainly to eliminate anomalies for flow through any radially drilled cavities. Although the alteration in the permeability due to heating is marginal, the changes could, in general, be irreversible.

The results of the permeability measurements involving heated samples can only be interpreted in the sense of an *average* temperature of 140 °C. From the point of view of applications of the results to nuclear waste disposal endeavors, where the reference temperatures are within 100 °C, the heating of the saturated granite and the associated development of pore fluid pressures within the fabric is *not* expected to substantially alter the pore fabric of the granite. This, however, does not rule out the possibility of long-term alterations in the permeability of the granite by thermally-induced processes such as creep, movements at grain boundaries and thermomechanical damage (in the form of microcracks and microvoids) that could result from stresses generated due to thermal loadings. The permeabilities measured in all the tests range from (1.6 to 4.0) $\times 10^{-19}$m$^2$. The results cited by KRANZ *et al.* (1979) for laboratory measured values of permeability for intact Barre granite range

Table 2

*Summary of results of permeability tests on intact granite*

| Test Set | Test Condition | No. of Tests | Permeability Range $K_i = (\text{const.})10^{-19}$ $(m^2)$ |
|---|---|---|---|
| 1 | Air dry granite cylinder I | 6 | 2.8 to 4.0 |
| 2 | Air dry granite cylinder I heated to 90 °C and cooled to ambient temperature | 6 | 2.2 to 2.5 |
| 3 | Air dry granite cylinder II heated to 90 °C and cooled to ambient temperature | 6 | 2.2 to 2.5 |
| 4 | Granite cylinder II subjected to fluid influx at 0.1 ml/min for 12 days | 6 | 2.0 to 3.0 |
| 5 | Granite Cylinder I subjected to pulse tests after 24 hours of constant flow saturation | 6 | 1.6 to 2.3 |
| 6 | Granite cylinder I subjected to an average temperature of 140 °C. Sample allowed to cool to 26 °C | 3 | 3.0 to 3.8 |
| 7 | Fully cooled granite cylinder I subjected to fluid influx at 0.1 ml/min for 12 days | 3 | 2.8 to 3.2 |

In all pulse tests, the fluid filled cavity is subjected to a pressure of 1.8 MPa, 1 hour prior to the test. The pressure at the start of a pulse test is 600 kPa.
The Test Sets 4 and 5, refer to results of pulse tests conducted after continuous flow at 600 kPa.
Note that the permeability estimates obtained from results of Test Sets 1, 2 and 3 can be only interpreted as "*Apparent permeability*" of the granite in an unsaturated condition.
The ambient temperature of the test facility is 23 °C.

from approximately $10^{-18}$ m$^2$ to $10^{-19}$ m$^2$. The results of TRIMMER *et al.* (1980) (in their Fig. 8), when linearly extrapolated to almost zero effective pressure, indicate that the permeability of the tested Westerly granite is of the order of $4 \times 10^{-19}$ m$^2$. BRACE (1984) indicates a value of $10^{-18}$ m$^2$ for crystalline rock. DETOURNAY and CHENG (1993) cite a value of $10^{-19}$ m$^2$ for Westerly granite. Thus, the results derived from the present investigation display consistency with other published data for permeability of crystalline rocks. In this sense, the experimental techniques, be it rectilinear pulse tests or radial flow pulse tests, can provide satisfactory estimates for the permeability of materials such as granite. Finally, it is natural to enquire whether the results of tests where nearly constant flow rates have been established (Figs. 9 and 13), could in any way be utilized to estimate the permeability of the granite. If we assume that a steady state of flow exists during these experiments the solution of Laplace's equation for the radial flow problem gives

$$K_i = \frac{Q\mu \ \ln(b/a)}{2\pi pL} \tag{33}$$

where $Q$ is the near-steady flow rate, $p$ is the cavity pressure at steady flow, $\mu$ is the dynamic fluid viscosity, $L$ is the height of the cylinder and $a$ and $b$ its respective inner and outer radii. The results of peak pressures at constant flow rates deduced from Fig. 9 and 13 are approximately 960 kPa and 800 kPa, respectively. These give permeability estimates of (1.21 and 1.46) $\times 10^{-18}$ m$^2$, respectively. These results are, in general, an order of magnitude higher than those derived from the pulse tests. *The reasons for this discrepency are not entirely clear*. It could be argued that by drilling the internal cavity in the cylinder, some local damage is induced in the granite, particularly in the vicinity of the cavity, representing an appreciable region of the granite participating in the pulse test. Such damage should invariably lead to an increase in the permeability of granite as derived from the pulse tests. In this case, however, the estimates based on the constant flow results indicate the reverse. The estimates for the permeability obtained from the current research investigation, however, vary between $1.2 \times 10^{-18}$ m$^2$ to $4.0 \times 10^{-19}$ m$^2$. These are within the range of values quoted in the literature for intact igneous geological materials such as granite.

The basic objective of the overall research program was to assess the importance of thermally-induced pore fluid pressure generation in saturated low permeability rock and the influence of such pressures on the development of micro-mechanical damage, which in turn can permanently alter the permeability characteristics of the material. Such permeability alterations are important to the definition of time scales associated with radionuclide migration from underground repositories for heat-emitting nuclear fuel wastes. From this point of view, it appears that thermal loadings in the range of 100 °C are insufficient to cause substantial micro-mechanical alterations in the short-term to influence the permeability of materials such as granite. Sustained temperatures even in this range can result in mineral dissolution and deposition that could in turn lead to permeability alterations. The effects of permeability reduction can also be a factor of some concern, since these are potential zones for hydraulic fracture generation in low permeability geomaterials.

## *Acknowledgements*

The authors would like to thank Dr. D.E. Moore of the U.S. Geological Survey, Menlo Park, California, and an anonymous reviewer for their critical evaluation of the manuscript, and for the highly constructive comments. The work presented in this paper was supported through Research Grants awarded by the Natural Sciences and Engineering Research Council of Canada and the Canadian Nuclear Safety Commission (CNSC). The authors are grateful to Mr. N. Vannelli for carrying out the experiments and to the scientists at CNSC for their valuable comments. One of the authors (APSS) would like to express his thanks to the Université Joseph Fourier

for a Visiting Professorship at the Laboratoire 3S, during which time the research was completed.

## References

Abramowitz, M.and Stegun, I.A. (1964) *Handbook of Mathematical Functions*, National Bureau of Standards, Applied Mathematics Series 55 (US Government Printing Office, Wash., D.C.,).

Ahmed, U., Crary, S.F., and Coates, G.R. (1991), *Permeability Estimation: The Various Sources and their Interrelationships*, J. Petrol. Tech. *43*, 578–587.

Ahola, M.P. (1995), *Expert Panel Review of CNWRA Coupled Thermal-Mechanical-Hydrological Processes Research Project,* Report CNWRA 95-02, Centre for Nuclear Regulatory Analysis, San Antonio, Texas.

Banthia, N. and Mindess, S. (1989), *Water Permeability of Cement Paste*, Cem. Conc. Res. *19,* 727–736.

Barenblatt, G.I., Entov, V.M., and Ryzhik, V.M. (1990) *Theory of Fluid Flows Through Natural Rocks* (Kluwer Academic Publishers, Dordrecht, The Netherlands).

Bear, J., Tsang, C.-F., and de Marsily, G. (eds.) (1993) *Flow and Contaminant Transport in Fractured Rock* (Academic Press, New York).

Berkowitz, B. (1989), *Boundary Conditions along Permeable Fracture Walls: Influence on Flow and Conductivity*, Water Resour. Res. *25,* 1919–1922.

Biot, M. (1941), *General Theory of Three-Dimensional Consolidation*, J. Appl. Phys., *12*, 155–164.

Brace, W.F. (1978), *A Note on Permeability Changes in Geological Material due to Stress*, Pure Appl. Geophys. *116,* 627–633.

Brace, W.F. (1980), *Permeability of Crystalline and Argillaceous Rocks*, Int. J. Rock Mech. Min. Sci. and Geomech. Abstr. *17,* 241–251.

Brace, W.F. (1984), *Permeability of Crystalline Rock: New in situ Measurements*, J. Geophys. Res. *89,* 4327–4330.

Brace, W.F., Walsh, J.B., and Frangos, W.T. (1968), *Permeability of Granite under High Pressure*, J. Geophys. Res. *73,* 2225–2236.

Bredehoeft, J.D. and Papadopulos, I.S. (1980), *A Method for Determining the Hydraulic Properties of Tight Formations*, Water Resour. Res. *15,* 233–238.

Butler, Jr., J.J. (1998), The Design, Performance and Analysis of Slug Tests (Lewis Publ., Boca Raton, Fla).

Carlsson, A. and Olsson, T. (1979), *Hydraulic Conductivity and its Stress Dependence, Proceed. Workshop on Low-Flow, Low-Permeability Measurements in Largely Impermeable Rocks*, OECD, Paris, 249–254.

Carslaw, H.S. and Jaeger, J.C. (1959), *Conduction of Heat in Solids* (Oxford University Press, Oxford).

Chapman, N.A. and McKinley, I.G. (1987), *The Geological Disposal of Nuclear Waste,* (John Wiley, New York)

Chapuis, R.P. (1998), *Overdamped Slug Test in Monitoring Wells: Review of Interpretation Methods with Mathematical, Physical, and Numerical Analysis of Storativity Influence*, Can. Geotech. J. *35,* 697–719.

Chapuis, R.P. and Chenaf, D. (1998), *Detecting a Hydraulic Short Circuit along a Monitoring Well with the Recovery Curve of a Pumping Test in a Confined Aquifer: Method and Example,* Can. Geotech. J. *35,* 790–800.

Collins, R.E. (1961) *Flow of Fluids Through Porous Materials* (Van Nostrand Reinhold, New York).

Cooper, H.H., Bredehoeft, J.D., and Papadopulos, I.S. (1967), *Response of a Finite Diameter Well to an Instantaneous Charge of Water*, Water Resour. Res. *3,* 263–269.

Coussy, O. (1995) *Mechanics of Porous Continua* (John Wiley, New York).

Davis, S.N. (1969) *Porosity and Permeability of Natural Materials*, In *Flow Through Porous Media* (R.J.M. De Wiest, ed.) (Academic Press, N.Y.), pp. 53–87.

DAW, G.P. (1971), *A Modified Hoek-Franklin Triaxial Cell for Rock Permeability Measurements*, Geotechnique *21,* 89–91.

DETOURNAY, E. and CHENG, A.H.-D. (1993) *Fundamentals of poroelasticity*. In *Comprehensive Rock Engineering* (J.A. Hudson, ed.) (Pergamon Press, New York) Chapter 5, Vol. 2, *Analysis and Design Methods,* pp. 113–171.

DULLIEN, F.A.L. (1992) *Porous Media: Fluid Transport and Pore Structures*, 2nd Ed. (Academic Press, New York).

FREEZE, R.A. and CHERRY, J.A. (1979) *Groundwater* (Prentice-Hall, Englewood Cliffs, N.J).

GNIRK, P. (1993), *OEDC/NEA International Stripa Project. Overview Volume II: Natural Barriers*, SKB, Stockholm, Sweden.

HAIMSON, B.C. and DOE, T.W. (1983), *State of Stress, Permeability and Fractures in the Precambrian Granite of Northern Illinois*, J. Geophys. Res. *88,* 7355–7371.

HARDY Jr., J.R. (1991), *Laboratory Tests Conducted on Barre Granite; Compressive Strength, Flexural Strength, Modulus of Rupture, Adsorption and Bulk Specific Gravity and Petrographic Analysis,* Department of Mining Engineering, Pennsylvania State University, PA.

HEILAND, J. (2003), *Permeability of Triaxially Compresssed Sandstone: Influence of Deformation and Strain on Permeability*, Pure Appl. Geophys. *160,* 889–908.

HEYSTEE, R. and ROEGIERS, J.C. (1981), *The Effect of Stress on the Primary Permeability of Rock Cores. A Facet of Hydraulic Fracturing*, Can. Geotech. J. *18,* 195–204.

HODGKINSON, D. and BARKER, J. (1985), *Specification of a Test Problem for HYDROCOIN Level 1 Case 1: Transient Flow from a Borehole in a Fractured Permeable Medium*, UKAEA-Harwell, Report AERE, R11574, Harwell, U.K.

HSIEH, P.A., TRACY, J.V., NEUZIL, C.E., BREDEHOEFT, J.D., and SILLIMAN, S.E. (1981), *A Transient Laboratory Method for Determining the Hydraulic Properties of "Tight Rocks." I. Theory*, Int. J. Rock Mech. Min. Sci. and Geomech. Abstr. *18,* 245–252.

HUDSON, J.A. (ed.) (1993) *Comprehensive Rock Engineering*, Vols. 1-5 (Pergamon Press, New York).

JACOB, C.E. (1940), *On the Flow of Water in an Elastic Artesian Aquifer*, Trans. Am. Geophys. Union *21,* 574–586.

JACOB, C.E. (1947), *Drawdown Test to Determine Effective Radius of Artesian Well*, Trans. Am. Soc. Civ. Engrs. *112,* 1047–1064.

JING, L., RUTQUIST, J., STEPHANSSON, O., TSANG, C-F., and KAUTSKY, F. (1993), *DECOVALEX B Mathematical Models of Coupled T-H-M Processes for Nuclear Waste Repositories,* Report of Phase I, Swedish Nuclear Power Inspectorate, Stockholm, Sweden.

JING, L., RUTQUIST, J., STEPHANSSON, O., TSANG, C-F., and KAUTSKY, F. (1994), *DECOVALEX B Mathematical Models for Coupled T-H-M Processes for Nuclear Waste Repositories*, Report of Phase II, Swedish Nuclear Power Inspectorate, Stockholm, Sweden.

JING, L., STEPHANSSON, O., TSANG, C.-F., KNIGHT, L.J., and KAUTSKY, F. (1999), *DECOVALEX II Project-Executive Summary*, Swedish Nuclear Power Inspectorate Stockholm, Sweden.

JOHNSON, L.H., LENEVEU, D.M., SHOESMITH, D.W., OSCARSON, D.W., GRAY, M.N., LEMIRE, R.J., and GARISTO, N.C. (1994a), *The Disposal of Canada's Nuclear Fuel Waste: The Vault Model for Postclosure Assessment*, AECL Research Report AECL-10714:COG-93-4, Whiteshell Laboratories, Pinawa, Manitoba.

JOHNSON, L.H., TAIT, J.C., SHOESMITH, D.W., CROSTHWAITE, J.L., and GRAY, M.N. (1994b), *The Disposal of Canada's Nuclear Fuel Waste: Engineered Barriers Alternatives*, AECL Research Report, AECL-10718:COG-93-8, Whiteshell Laboratories, Pinawa, Manitoba.

KNUTSON, C.F. and BOHOR, B.F. (1963), *Reservoir Rock Behaviour under Moderate Confining Pressure*, Fifth Symposium on Rock Mechanics, University of Minnesota, MN, (Macmillan, N.Y.) pp. 627–659.

KRANZ, R.L., FRANKEL, A.D., ENGELDER, T., and SCHOLZ, C.H. (1979), *The Permeability of Whole and Jointed Barre Granite*, Int. J. Rock Mech. Min. Sci. and Geomech. Abstr. *16,* 225–234.

KUMPEL, H.-J. (ed.) (2000), *Thermo-hydro-mechanical Coupling in Fractured Rock*, Proc. 3rd Eurocon-ference on Rock Physics and Rock Mechanics, (Bad Honnef, Germany).

LAUGHTON, A.S., ROBERTS, L.E.J., WILKINSON, D., and GRAY, D.A. (1986), *The Disposal of Long-lived and Highly Radioactive Wastes*, Proc. Royal Society Discussion Meeting, Royal Society, London.

McNamee, J. and Gibson, R.E. (1960), *Displacement Functions and Linear Transforms Applied to Diffusion through Porous Elastic Media*, Quart. J. Mech. Appl. Math. *13,* 98–111.

Moore, D.E., Morrow, C.A., and Byerlee, J.D. (1983), *Chemical Reactions Accompanying Fluid Flow through Granite held in a Temperature Gradient*, Geochimica et Cosmochimica Acta, *47,* 445–453.

Morrow, C.A., Lockner, D., Moore, D., and Byerlee, J. (1981), *Permeability of Granite in a Temperature Gradient*, J. Geophys. Res. *80,* 3002–3008.

Morrow, C.A., Moore, D.E., and Lockner, D.A. (2001) *Permeability Reduction in Granite under Hydrothermal Conditions*, J. Geophys. Res. *106,* 30,551–30,560.

Nield, D.A. and Bejan, A. (1999) *Convection in Porous Media* (Springer-Verlag, Berlin).

Nguyen, T.S. and Selvadurai, A.P.S. (1995), *Coupled Thermal-mechanical-hydrological Behavior of Sparsely Fractured Rock: Implications for Nuclear Fuel Waste Disposal*, Int. J. Rock Mech. Min. Sci. and Geomech. Abstr. *32,* 465–479.

Nguyen, T.S. and Selvadurai, A.P.S. (1998), *A Model for Coupled Mechanical and Hydraulic Behaviour of a Rock Joint*, Int. J. Num. Analyt. Meth. Geomech. *22,* 29–48.

Oelkers, E.H. (1996), *Physical and Chemical Properties of Rocks and Fluids for Chemical Mass Transport Calculations*, Chapter 3 in *Reactive Transport in Porous Media* (P.C. Lichtner, C.I. Steefel and E.H. Oelkers, eds.), *Reviews in Mineralogy*, Mineralogical Society of America *34,* 131–191.

Papadopulos, I.S., Bredehoeft, J.D., and Cooper, H.H. (1973), *On the Analysis of "Slug Test" Data*, Water Resour. Res. *9,* 1087–1089.

Philips, O.M. (1991) *Flow and Reactions in Permeable Media* (Cambridge University Press, Cambridge).

Poon, C.S., Clark, A.I., Perry, R., Barker, A.P., and Barnes, P. (1986), *Permeability of Portland Cement Based Solidification Process for the Disposal of Hazardous Wastes*, Cem. Conc. Res. *9,* 1087–1089.

Rehbinder, G. (1996a), *The Double Packer Permeameter with Narrow Packers: Analytical Solution for Non-steady Flow*, Appl. Sci. Res. *56,* 255–279.

Rehbinder, G. (1996b), *The Double Packer Permeameter with Long Packers: An Approximate Analytical Solution*, Appl. Sci. Res. *56,* 281–297.

Rice, J.R. and Cleary, M.P. (1976), *Some Basic Stress Diffusion Solutions for Fluid Saturated Porous Media with Compressible Constituents*, Rev. Geophys. Space Phys. *14*, 227–241.

Rutquist, J. (1995), *Determination of Hydraulic Normal Stiffness of Fractures in Hard Rock from Well Testing*, Int. J. Rock Mech. Min. Sci. and Geomech. Abstr. *32,* 513–523.

Selvadurai, A.P.S. (ed.) (1996a) *Mechanics of Poroelastic Media*, (Kluwer Academic Publishers, Dordrecht, The Netherlands).

Selvadurai, A.P.S. (1996b), *Heat-induced Moisture Movement in a Clay Barrier. I. Experimental Modelling of Borehole Emplacement*, Engng. Geol. *41,* 239–256.

Selvadurai, A.P.S. (1996c), *Heat-induced Moisture Movement in a Clay Barrier. II. Computational Modelling and Comparison with Experimental Results*, Engng. Geol. *41,* 219–238.

Selvadurai, A.P.S. (1997), *Thermal Consolidation Effects around a High Level Repository*, Report No. RSP-0029, Atomic Energy Control Board of Canada, Ottawa, Canada.

Selvadurai, A.P.S., (2000) *Partial Differential Equations in Mechanics*. Vol. 1. *Fundamentals, Laplace's Equation, Diffusion Equation, Wave Equation* (Springer-Verlag, Berlin).

Selvadurai, A.P.S. and Carnaffan, P. (1997), *A Transient Pressure Pulse Technique for the Measurement of Permeability of a Cement Grout*, Can. J. Civ. Eng. *24,* 489–502.

Selvadurai, A.P.S. and Nguyen, T.S. (1995), *Computational Modelling of Isothermal Consolidation of Fractured Porous Media*, Comp. and Geotech. *17,* 39–73.

Selvadurai, A.P.S. and Nguyen, T.S. (1996), *Scoping Analyses for the Coupled Thermal-hydrological-mechanical Behaviour of the Rock Mass around a Nuclear Waste Repository*, Engng. Geol. *47,* 379–400.

Shmonov, V.M., Vitovtova, V.M., and Zarubina, I.V. (1994) *Permeability of Rocks at Elevated Temperatures and Pressures*. In *Fluids in the Crust; Equilibrium and Transport Properties* (Chapman and Hall, London), pp. 285–313.

Simmons, G.R. and Baumgartner, P. (1994), *The Disposal of Canada's Nuclear Fuel Waste: Engineering for a Disposal Facility,* AECL Research Report AECL-10715:COG-93-5, Whiteshell Laboratories, Pinawa, Manitoba.

STEPHANSSON, O. (ed.) (1995), *Special Issue on Thermo-Hydro-Mechanical Coupling in Rock Mechanics*, Int. J. Rock Mech. Min. Sci. and Geomech. Abstr. *32,* 389–535.

STEPHANSSON, O., JING, L., and TSANG, C.-F. (eds.) (1996), *Coupled Thermo-hydro-mechanical Properties of Fractured Media: Mathematical and Experimental Studies*, Developments in Geotech. Engin., *79* (Elsevier, Amsterdam).

SUMMERS, R., WINKLER, K., and BYERLEE, J.D. (1978), *Permeability Changes during the Flow of Water through Westerly Granite at Temperatures of 100°–400* °C, J. Geophys. Res. *83,* 339–344.

TSANG, C.-F. (ed.) (1987) *Coupled Processes Associated with Nuclear Waste Repositories* (Academic Press, New York).

TSANG, C.-F. (1991) *Coupled Thermomechanical Hydrochemical Processes in Rock Fractures*, Rev. Geophys. *29,* 537–551.

TRIMMER, D., BONNER, B., HEARD, H.C., and DUBA, A. (1980), *Effect of Pressure and Stress on Water Transport in Intact and Fractured Gabbro and Granite*, J. Geophys. Res. *85*, 7059–7071.

VAN EVERDINGEN, A.F. and HURST, W. (1949), *The Application of Laplace Transformation to Flow Problems in Reservoirs*, Trans. AIME *186,* 305–324.

VAUGHN, P.J. (1989) *Analysis of Permeability Reduction during Flow of Heated Aqueous Fluid through Westerly Granite* In *Coupled Processes Associated with Nuclear Waste Repositories* (C.-F. Tsang, ed.) (Academic Press, New York), pp. 529–539.

VITOVTOVA, V.M. and SHMONOV, V.M. (1982), *Permeability of Rocks at Pressures to 2000 kg/cm$^2$ and Temperatures to 600* °C, Dokl. Akad. Nauk. SSR *266,* 1244–1248.

WANG, J.S.Y., NARASIMHAN, T.N., TSANG, C.-F., and WITHERSPOON, P.A. (1977), *Transient Flow in Tight Fractures*, *Proc. Invitational Well Testing Symposium*, Lawrence Berkeley Lab. Report LBL 7027, pp. 103–116.

WATSON, G.N. (1944) *A Treatise on the Theory of Bessel Functions*, 2nd Edition (Cambridge University Press, Cambridge).

WU, Y.-S. and PRUESS, K. (2000), *Integral Solutions for Transient Fluid Flow through a Porous Medium with Pressure-Dependent Permeability*, Int. J. Rock Mech. Min. Sci. and Geomech. Abstr. *37,* 51–61.

ZARAISKY, G.P. and BALASHOV, V.N. (1994), *Thermal decompaction of rocks.* In *Fluids in the Crust: Equilibrium and Transport Properties* (Chapman and Hall, London), pp. 253–284.

ZOBACK, M.D. and BYERLEE, J.D. (1975), *The Effect of Microcrack Dilatancy on the Permeability of Westerly Granite*, J. Geophys. Res. *80,* 752–755.

ZONOV, S.V., ZARAISKY, G.P., and BALASHOV, V.N. (1989), *The Effect of Thermal Decompaction on Permeability of Granites with Lithostatic Pressures being Slightly in Excess of Fluid Pressure,* Dokl. Akad. Nauk. SSR *307,* 191–195.

(Received May 27, 2003, accepted December 12, 2003)